

Underdetermined 2D-DOD and 2D-DOA Estimation for Bistatic Coprime EMVS-MIMO Radar: From the Difference Coarray Perspective

Qianpeng XIE, Yihang DU, He WANG, Xiaoyi PAN, and Feng ZHAO

Abstract

In this paper, the underdetermined 2D-DOD and 2D-DOA estimation for bistatic coprime EMVS-MIMO radar is considered. Firstly, a 5-D tensor model was constructed by using the multi-dimensional space-time characteristics of the received data. Then, an 8-D tensor has been obtained by using the auto-correlation calculation. To obtain the difference coarrays of transmit and receive EMVS, the decoupling process between the spatial response of EMVS and the steering vector is inevitable. Thus, a new 6-D tensor can be constructed via the tensor permutation and the generalized tensorization of the canonical polyadic decomposition. According to the theory of the Tensor-Matrix Product operation, the duplicated elements in the difference coarrays can be removed by the utilization of two designed selection matrices. Due to the centrosymmetric geometry of the difference coarrays, two DFT beamspace matrices were subsequently designed to convert the complex steering matrices into the real-valued ones, whose advantage is to improve the estimation accuracy of the 2D-DODs and 2D-DOAs. Afterwards, a third-order tensor with the third-way fixed at 36 was constructed and the Parallel Factor algorithm was deployed, which can yield the closed-form automatically paired 2D-DOD and 2D-DOA estimation. The

This work was supported in part by the National Natural Science Foundation of China under Grant 61890545, 61890542 and 61890540. Qianpeng XIE, Xiaoyi PAN, Feng ZHAO are with the State Key Laboratory of Complex Electromagnetic Environment Effects on Electronics and Information System, National University of Defense Technology, Changsha 410073, China(email:13721038905@163.com, mrpanxy@nudt.edu.cn, zhfbec@tom.com). Yihang DU is with the Sixty-Third Research Institute, National University of Defense Technology, Nanjing 210007, China(email:dyhcs11991@163.com). He WANG is with the School of Electronic Science, National University of Defense Technology, Changsha 410073, China.(email:hw8g16@soton.ac.uk)(Corresponding author: Qianpeng XIE)

Manuscript received April 19, 2005; revised August 26, 2015.

simulation results show that the proposed algorithm can exhibit superior estimation performance for the underdetermined 2D-DOD and 2D-DOA estimation.

Index Terms

Bistatic coprime EMVS-MIMO radar, 2D-DOD and 2D-DOA estimation, difference coarrays, high-order tensor model, PARAFAC algorithm

I. INTRODUCTION

Studies about the electromagnetic vector sensors (EMVS) have attracted extensive attention due to their excellent measurement capabilities of angle parameters and polarization parameters [1]-[5]. Compared with the scalar array, EMVS with three orthogonal electric dipoles and three orthogonal magnetic dipoles can obtain the electromagnetic field vector information of the targets. Recently, in order to measure the polarization information of targets in bistatic MIMO radars, the EMVS has been used as the transmit and receive array in the bistatic MIMO radar system.

For the achievement of multi-dimensional parameter estimation in bistatic EMVS-MIMO radar, the ESPRIT algorithm was firstly proposed in [6]. But, this algorithm has high computational complexity due to the singular value decomposition on the covariance matrix of the array received data. In [7], a computationally friendly PM estimator was proposed to construct the virtual direction matrix for bistatic EMVS-MIMO radar. In [8], a tensor subspace based algorithm has been developed to improve the estimated performance by exploiting the inherent multi-dimensional structure of the received data. Additional optimization process in [6]-[8] is inevitable because of the pair matching between 2D-DOD and 2D-DOA. Thus, an improved PM algorithm in [9] has been raised to realize the automatic pair of 2D-DOD and 2D-DOA, and this method can further decrease the computational complexity. The disadvantage of the PM algorithms in [7] and [9] is the relatively poor estimation performance. In [10], the PARAFAC algorithm was utilized to realize the automatically paired 2D-DOD and 2D-DOA estimation. In [11], the bistatic coprime EMVS-MIMO radar was designed to enhance the 2D-DOD and 2D-DOA estimation performance.

It is apparent that the above-mentioned algorithms do not utilize the inherent difference coarray of transmit and receive EMVS, when conducting multi-dimensional parameter estimation in bistatic EMVS MIMO radar. According to [12]-[17], the difference coarray of the original array can offer larger array apertures, which means that the underdetermined DOA estimation is obtain-

able. For bistatic EMVS-MIMO radar, the challenge for constructing the difference coarray of the transmit and receive EMVS is the coupling in the spatial response alongside the steering vector. In this paper, the de-coupling process has been completed with the help of tensor operation. To estimate more targets than elements, the difference coarray of transmit and receive EMVS has been attained by the high order tensor permutation along with the generalized tensoriation of the canonical polyadic decomposition. In addition, two designed selection matrices have been used to remove the repeated elements in the difference coarray via the Tensor-Matrix product rule. The geometry of the difference coarray for both transmit and receive EMVS exhibit centrosymmetry. As discussed in [22]-[26], the DFT beamspace matrix can be exploited to convert the complex array manifold matrix with centro-symmetric structure into the real-value one. This process can enhance the 2D-DOD and 2D-DOA estimation performance in the bistatic EMVS-MIMO radar. Besides, a third-order tensor has been constructed with the dimension of the third-way fixed at 36. Finally, The automatically paired transmit/receive elevation angle, transmit/receive azimuth angle, transmit/receive polarization angle and transmit/receive polarization phase difference can be accurately derived from the estimated transmit and receive factor matrices acquired by the PARAFAC algorithm. Simulation results have verified its effectiveness.

The paper is organized as follows. Section II describes the nomenclature employed in this publication. Section III formulates the signal model of the bistatic coprime EMVS-MIMO radar. Section IV reports the detailed derivation process of the proposed algorithm. Section V presents simulations to verify the effectiveness of the proposed algorithm. Section VI provides a summary.

II. NOMENCLATURE

- \mathbf{A}^* : The complex conjugate of \mathbf{A}
- \mathbf{A}^T : The transpose of \mathbf{A}
- \mathbf{A}^H : The Hermitian transpose of \mathbf{A}
- \mathbf{A}^{-1} : The inverse of \mathbf{A}
- \mathbf{A}^\dagger : The pseudo-inverse of \mathbf{A}
- $\mathbf{a} \otimes \mathbf{b}$: The Kronecker product of \mathbf{a} and \mathbf{b}
- $\mathbf{A} \odot \mathbf{B}$: The Khatri-Rao product of \mathbf{A} and \mathbf{B}
- $\mathbf{A} \oplus \mathbf{B}$: The Hadamard product of \mathbf{A} and \mathbf{B}
- $\mathbf{a} \circ \mathbf{b}$: The vector outer product of \mathbf{a} and \mathbf{b}
- $\mathbf{a} \times \mathbf{b}$: The vector-cross-product of \mathbf{a} and \mathbf{b}

- $(\mathbf{II})_{\mathbf{A}}^{\perp}$: The projection matrix of the matrix \mathbf{A}
- $\sin(\theta)$: The sine of θ
- $\cos(\theta)$: The cosine of θ
- $\tan(\theta)$: The tangent of θ
- $\arcsin(\theta)$: The inverse sine of θ
- $\arccos(\theta)$: The inverse cosine of θ
- $\arctan(\theta)$: The inverse tangent of θ
- $\angle(\mathbf{a})$: The phase angles of \mathbf{a}
- $\text{real}(\mathbf{A})$: The real part of \mathbf{A}
- $\min[a, b]$: smaller value taken from a or b .
- $\mathcal{D}_i(\mathbf{A})$: The diagonal matrix with the i -th colume elements from \mathbf{A} .
- \mathbf{I}_N : The $N \times N$ identity matrix
- $\mathbf{0}_N$: The $N \times N$ matrix of zeros.
- $\mathbf{1}_N$: The $N \times N$ matrix of ones.
- $\kappa_{\mathbf{A}}$: The κ -rank of \mathbf{A} .
- **Some Definations of Coprime Array in [12]-[13]**

Definition 1 (\mathbb{D} , Difference Coarray). For a sparse coprime array specified by an integer set \mathbb{S} , its difference coarray \mathbb{D} is defined as

$$\mathbb{D} = \{n_1 - n_2 | n_1, n_2 \in \mathbb{S}\} \quad (1)$$

Definition 2 (\mathbb{U} , maximum central contiguous ULA). Let \mathbb{S} denote a coprime array and \mathbb{D} be its difference coarray. The maximum central contiguous ULA segment in \mathbb{D} is

$$\mathbb{U} = \{m | -|m|, \dots, -1, 0, 1, \dots, |m|\} \quad (2)$$

Definition 3 (\mathbb{W} , Weight Functions). The weight function $w(m)$ of an array \mathbb{S} is defined as the number of sensor pairs that lead to coarray index m , i.e., $|\{(n_1, n_2 \in \mathbb{S}^2) | n_1 - n_2 = m\}|$

- **Some Definations of Tensor in [18]-[21]**

Definition 4 (Mode- n Tensor-Matrix Product). The mode- n product of an N -order tensor

set $\mathcal{X} \in \mathbb{C}^{I_1 \times I_2 \times \dots \times I_N}$ and a matrix $\mathbf{A} \in \mathbb{C}^{J_n \times I_n}$ is defined as

$$\mathcal{Y} = \mathcal{X} \times_n \mathbf{A} \in \mathbb{C}^{I_1 \times \dots \times I_{n-1} \times J_n \times I_{n+1} \times \dots \times I_N} \quad (3)$$

Definition 5 (Outer product of two tensors). The outer product of two tensors $\mathcal{A} \in \mathbb{C}^{I_1 \times I_2 \times \dots \times I_N}$ and $\mathcal{B} \in \mathbb{C}^{J_1 \times J_2 \times \dots \times J_M}$ is defined as

$$\mathcal{Y} = \mathcal{A} \circ \mathcal{B} \in \mathbb{C}^{I_1 \times \dots \times I_N \times J_1 \times J_2 \times \dots \times J_M} \quad (4)$$

whose elements are $y_{i_1, i_2, \dots, i_N, j_1, j_2, \dots, j_M} = a_{i_1, i_2, \dots, i_N} \cdot b_{j_1, j_2, \dots, j_M}$

Definition 6 (PARAFAC decomposition). For an N th-order tensor $\mathcal{X} \in \mathbb{C}^{I_1 \times I_2 \times \dots \times I_N}$, it can be expressed as a linear combination of rank-1 tensors as follows:

$$\mathcal{X} = \sum_{k=1}^K \mathbf{a}_{k1} \circ \mathbf{a}_{k2} \circ \dots \circ \mathbf{a}_{kN} \quad (5)$$

where $\mathbf{a}_{kn} \in \mathbb{C}^{I_n \times 1}$, $k = 1, 2, \dots, K$ denotes the rank-1 tensor.

Definition 7 (Generalized Tensorization of a PARAFAC model). For an N th-order PARAFAC model $\mathcal{A} = \sum_{k=1}^K \mathbf{a}_{k1} \circ \mathbf{a}_{k2} \circ \dots \circ \mathbf{a}_{kN} \in \mathbb{C}^{I_1 \times I_2 \times \dots \times I_N}$ with $\mathbf{a}_{nk} \in \mathbb{C}^{I_n}$ ($n = 1, \dots, N$), let the ordered sets $\mathbb{A}_j = [r_{j,1}, r_{j,2}, \dots, r_{j,L_j}]$ for $j = 1, 2, \dots, J$ be a partitioning of the dimensions $\mathbb{A} = [1, 2, \dots, N]$, the generalized tensorization of \mathcal{A} is defined as

$$\begin{aligned} \mathcal{A}_{\mathbb{A}_1, \mathbb{A}_2, \dots, \mathbb{A}_J} &= \sum_{k=1}^K \mathbf{b}_{1k} \circ \mathbf{b}_{2k} \circ \dots \circ \mathbf{b}_{Jk} \\ &\in \mathbb{C}^{I_{R_1} \times I_{R_2} \times \dots \times I_{R_J}} \end{aligned} \quad (6)$$

where $I_{R_j} = \prod_{l=1}^{L_j} I_{r_{j,l}}$ and $\mathbf{b}_{jk} = \mathbf{a}_{r_{j,L_j}} \otimes \mathbf{a}_{r_{j,L_j-1}} \otimes \dots \otimes \mathbf{a}_{r_{j,1}}$.

III. DATA MODEL

A bistatic coprime EMVS-MIMO radar system with M transmit EMVS and N receive EMVS is demonstrated in Fig. 1. Let the array positions of transmit EMVS and receive EMVS are \mathbf{L}_t and \mathbf{L}_r , respectively

$$\mathbf{L}_t = \{M_1 m_2 | 0 \leq m_2 \leq M_2 - 1\} \cup \{M_2 m_1 | 0 \leq m_1 \leq 2M_1 - 1\} \quad (7)$$

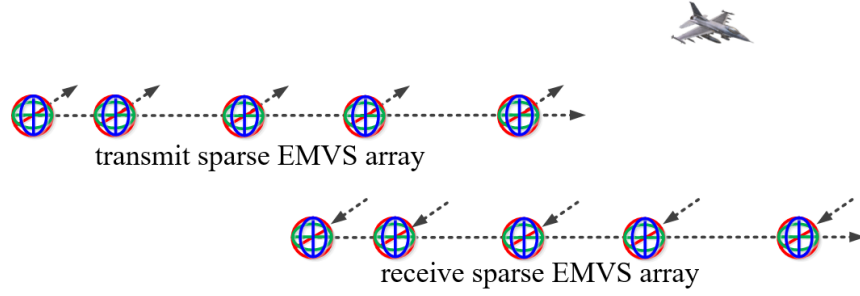


Fig. 1. Bistatic coprime EMVS-MIMO radar system.

$$\mathbf{L}_r = \{N_1 n_2 | 0 \leq n_2 \leq N_2 - 1\} \cup \{N_2 n_1 | 0 \leq n_1 \leq 2N_1 - 1\} \quad (8)$$

Assuming the number of targets is K , the transmit steering vector and receive steering vector of the bistatic coprime EMVS-MIMO radar can be expressed as

$$\mathbf{c}_{t_k} = \mathbf{a}_{t_k} \otimes \mathbf{q}_{t_k}(\theta_{t_k}, \phi_{t_k}, \gamma_{t_k}, \eta_{t_k}) \quad (9)$$

$$\mathbf{c}_{r_k} = \mathbf{a}_{r_k} \otimes \mathbf{q}_{r_k}(\theta_{r_k}, \phi_{r_k}, \gamma_{r_k}, \eta_{r_k}) \quad (10)$$

where $\theta_{t_k}, \theta_{r_k} \in [0, \pi)$, $\phi_{t_k}, \phi_{r_k} \in [0, 2\pi)$, $\gamma_{t_k}, \gamma_{r_k} \in [0, \pi/2)$ and $\eta_{t_k}, \eta_{r_k} \in [-\pi, \pi)$ denote the transmit/receive elevation angle, transmit/receive azimuth angle, transmit/receive polarization angle and transmit/receive polarization phase difference, respectively. $\mathbf{q}_{t_k}(\theta_{t_k}, \phi_{t_k}, \gamma_{t_k}, \eta_{t_k})$ and $\mathbf{q}_{r_k}(\theta_{r_k}, \phi_{r_k}, \gamma_{r_k}, \eta_{r_k})$ represent the spatial response of the transmit EMVS and the receive EMVS of the k -th target, respectively. $\mathbf{a}_{t_k} = [e^{-j2\pi d_{t0} \sin(\theta_{t_k})}, \dots, e^{-j2\pi d_{tM} \sin(\theta_{t_k})}]^T$, $\mathbf{a}_{r_k} = [e^{-j2\pi d_{r0} \sin(\theta_{r_k})}, \dots, e^{-j2\pi d_{rN} \sin(\theta_{r_k})}]^T$. For an EMVS, the spatial response \mathbf{q} can be expressed as

$$\mathbf{q}(\theta, \phi, \gamma, \eta) = \underbrace{\begin{bmatrix} \cos(\phi) \cos(\theta) & -\sin(\phi) \\ \sin(\phi) \cos(\theta) & \cos(\phi) \\ -\sin(\theta) & 0 \\ -\sin(\phi) & -\cos(\phi) \cos(\theta) \\ \cos(\phi) & -\sin(\phi) \cos(\theta) \\ 0 & \sin(\theta) \end{bmatrix}}_{\mathbf{F}(\theta, \phi)} \underbrace{\begin{bmatrix} \sin(\gamma) e^{j\eta} \\ \cos(\gamma) \end{bmatrix}}_{\mathbf{g}(\gamma, \eta)} \quad (11)$$

where $\mathbf{F}(\theta, \phi) \in \mathbb{C}^{6 \times 2}$ denotes the spatial angular location matrix, $\mathbf{g}(\gamma, \eta) \in \mathbb{C}^{2 \times 1}$ is representative of the polarization states vector.

According to [1], the elevation angle θ and azimuth angle ϕ can be extracted from the normalized Poynting vector of $\mathbf{q}(\theta, \phi, \gamma, \eta)$

$$\begin{bmatrix} u \\ v \\ w \end{bmatrix} \triangleq \frac{\mathbf{q}_{[1,2,3]}}{\|\mathbf{q}_{[1,2,3]}\|} \times \frac{\mathbf{q}_{[4,5,6]}^*}{\|\mathbf{q}_{[4,5,6]}\|} = \begin{bmatrix} \sin(\theta) \cos(\phi) \\ \sin(\theta) \sin(\phi) \\ \cos(\theta) \end{bmatrix} \quad (12)$$

By using the orthogonality of the bistatic coprime EMVS-MIMO radar transmit and receive waveforms, the signal model after matched filtering at the receive front can be denoted as

$$\mathbf{y}(t) = ((\mathbf{A}_t \odot \mathbf{Q}_t) \odot (\mathbf{A}_r \odot \mathbf{Q}_r))\mathbf{s}(t) + \mathbf{n}(t) \quad (13)$$

where $\mathbf{A}_t = [\mathbf{a}_{t_1} \ \mathbf{a}_{t_2} \ \cdots \ \mathbf{a}_{t_K}]$, $\mathbf{A}_r = [\mathbf{a}_{r_1} \ \mathbf{a}_{r_2} \ \cdots \ \mathbf{a}_{r_K}]$, $\mathbf{Q}_t = [\mathbf{q}_{t_1} \ \mathbf{q}_{t_2} \ \cdots \ \mathbf{q}_{t_K}]$ and $\mathbf{Q}_r = [\mathbf{q}_{r_1} \ \mathbf{q}_{r_2} \ \cdots \ \mathbf{q}_{r_K}]$ denote the transmit steering matrix, the receive steering matrix, the transmit spatial response matrix and the receive spatial response matrix, respectively. For the total L snapshots, the sample data can be further derived as

$$\mathbf{Y} = ((\mathbf{A}_t \odot \mathbf{Q}_t) \odot (\mathbf{A}_r \odot \mathbf{Q}_r))\mathbf{S} + \mathbf{N} \quad (14)$$

For the bistatic coprime EMVS-MIMO radar with M -element transmit EMVS and N -element receive EMVS, the matrix dimension of $(\mathbf{C}_t \odot \mathbf{C}_r)$ is $\mathbb{C}^{36MN \times K}$. In order to achieve the underdetermined 2D-DOD and 2D-DOA, the difference coarray of the transmit EMVS and receive EMVS will be deployed to construct a new third-order tensor model. Moreover, from (14), it can be seen that the received data \mathbf{Y} satisfies the space-time multi-dimensional tensor structure.

Here, some assumptions are made in order to effectively estimate the transmit 4-D parameter $(\boldsymbol{\theta}_t, \boldsymbol{\phi}_t, \boldsymbol{\gamma}_t, \boldsymbol{\eta}_t)$ and receive 4-D parameter $(\boldsymbol{\theta}_r, \boldsymbol{\phi}_r, \boldsymbol{\gamma}_r, \boldsymbol{\eta}_r)$,

- The value of $(\boldsymbol{\theta}_t, \boldsymbol{\phi}_t, \boldsymbol{\gamma}_t, \boldsymbol{\eta}_t)$ and $(\boldsymbol{\theta}_r, \boldsymbol{\phi}_r, \boldsymbol{\gamma}_r, \boldsymbol{\eta}_r)$ should satisfy $\boldsymbol{\theta}_t, \boldsymbol{\theta}_r \in [0, \pi/2)$, $\boldsymbol{\phi}_t, \boldsymbol{\phi}_r \in [0, \pi/2)$, $\boldsymbol{\gamma}_t, \boldsymbol{\gamma}_r \in [0, \pi/2)$, $\boldsymbol{\eta}_t, \boldsymbol{\eta}_r \in [0, \pi/2)$.
- The signals are stationary, non-Gaussian random process and statistically independent of each other.
- The number of signals K is known or corrected estimated by the existing algorithm.
- The \mathbf{N} is zero-mean, complex Gaussian white noise.
- The noise is statistically independent of the signals.

IV. THE PROPOSED DIFFERENCE COARRAY STRATEGY

A. Construction of the Difference Coarray

For the estimation of more targets than elements, the difference coarray of transmit and receive EMVS are constructed. From (9) and (10), it can be found that \mathbf{a}_{tk} and \mathbf{q}_{tk} , \mathbf{a}_{rk} and \mathbf{q}_{rk} are copuling, respectively. Therefore, in order to obtain the difference coarrays, the de-coupling is invetiable.

To reserve the mutiple space-time structure in \mathbf{Y} , a 5-D tensor \mathcal{Y} can be constructed as

$$\mathcal{Y} = \sum_{k=1}^K \mathbf{a}_{tk} \circ \mathbf{q}_{tk} \circ \mathbf{a}_{rk} \circ \mathbf{q}_{rk} \circ \mathbf{s}_k + \mathcal{N}_l \quad (15)$$

Then, a 8-D tensor \mathcal{R} can be obtained via the following correlation operation between \mathcal{Y} and \mathcal{Y}^*

$$\mathcal{R} = \mathbf{E}[\mathcal{Y} \circ \mathcal{Y}^*] = \sum_{k=1}^K \sigma_k^2 \underbrace{\mathbf{a}_{tk}}_1 \circ \underbrace{\mathbf{q}_{tk}}_2 \circ \underbrace{\mathbf{a}_{rk}}_3 \circ \underbrace{\mathbf{q}_{rk}}_4 \circ \underbrace{\mathbf{a}_{tk}^*}_5 \circ \underbrace{\mathbf{q}_{tk}^*}_6 \circ \underbrace{\mathbf{a}_{rk}^*}_7 \circ \underbrace{\mathbf{q}_{rk}^*}_8 + \mathcal{R}_N \quad (16)$$

where $\sigma_k^2, k = 1, 2, \dots, K$ denotes the power of the k -th source. And, according to **Definition 1**, the corrsponding difference coarray of transmit EMVS and receive EMVS can be obtained by combining the factor vectors \mathbf{a}_{tk} and \mathbf{a}_{tk}^* , \mathbf{a}_{rk} and \mathbf{a}_{rk}^* , respectively. Thus, the factor vectors can be rearranged as $[1, 2, 3, 4, 5, 6, 7, 8] \mapsto [1, 5, 2, 3, 7, 4, 6, 8]$ based on the tensor permutation rule, and a new 8-D \mathcal{R}_1 can be expressed as

$$\begin{aligned} \mathcal{R}_1 &= \sum_{k=1}^K \sigma_k^2 \underbrace{\mathbf{a}_{tk}}_1 \circ \underbrace{\mathbf{a}_{tk}^*}_5 \circ \underbrace{\mathbf{q}_{tk}}_2 \circ \underbrace{\mathbf{a}_{rk}}_3 \circ \underbrace{\mathbf{a}_{rk}^*}_7 \circ \underbrace{\mathbf{q}_{rk}}_4 \circ \underbrace{\mathbf{q}_{tk}^*}_6 \circ \underbrace{\mathbf{q}_{rk}^*}_8 + \mathcal{R}_{N1} \\ &= \sum_{k=1}^K \sigma_k^2 \underbrace{\mathbf{a}_{tk}}_1 \circ \underbrace{\mathbf{a}_{tk}^*}_2 \circ \underbrace{\mathbf{q}_{tk}}_3 \circ \underbrace{\mathbf{a}_{rk}}_4 \circ \underbrace{\mathbf{a}_{rk}^*}_5 \circ \underbrace{\mathbf{q}_{rk}}_6 \circ \underbrace{\mathbf{q}_{tk}^*}_7 \circ \underbrace{\mathbf{q}_{rk}^*}_8 + \mathcal{R}_{N1} \end{aligned} \quad (17)$$

Then, the indeces 1 and 2, 4 and 5, 7 and 8 need to be combined by the use of the generalized tensorization of the canonical polyadic decomposition in **Definition 7**. As a result, a new 5-D tensor $\mathcal{R}_2 = \mathcal{R}_{1[1,2][4,5][7,8]}$ can be achieved as

$$\mathcal{R}_2 = \sum_{k=1}^K \sigma_k^2 \tilde{\mathbf{a}}_{tk} \circ \mathbf{q}_{tk} \circ \tilde{\mathbf{a}}_{rk} \circ \mathbf{q}_{rk} \circ \tilde{\mathbf{q}}_k + \mathcal{R}_{N2} \quad (18)$$

where $\tilde{\mathbf{a}}_{tk} = \mathbf{a}_{tk} \otimes \mathbf{a}_{tk}^*$, $\tilde{\mathbf{a}}_{rk} = \mathbf{a}_{rk} \otimes \mathbf{a}_{rk}^*$, $\tilde{\mathbf{q}}_k = \mathbf{q}_{tk}^* \otimes \mathbf{q}_{rk}^*$.

According to **Definition 1**, for the M transmit coprime EMVS with the number of the first subarray is $M1$ and the second subarray is $M2$, the N transmit coprime EMVS with the number

of the first subarray is N_1 and the second subarray is N_2 , the number of continue virtual array elements in the corresponding difference coarrays can be deonted as

$$\widetilde{M} = 2M_1M_2 + 2M_1 + 1 \quad (19)$$

$$\widetilde{N} = 2N_1N_2 + 2N_1 + 1 \quad (20)$$

However, the difference coarrays of the coprime transmit array and the coprime receive array contain many duplicated elements. To attain the maximum central contiguous ULA in the difference coarrays, it is necessary to remove the repeated elements, which can be realized by the application of tensor matrix product rules. Two selection matrices \mathbf{J}_1 and \mathbf{J}_2 are designed on the basis of **Algorithm 1**. So, a new 6-D tensor can be expressd as

$$\begin{aligned} \mathcal{R}_3 &= \mathcal{R}_2 \times_1 \mathbf{J}_1 \times_3 \mathbf{J}_2 \\ &= \sum_{k=1}^K \sigma_k^2 \widetilde{\mathbf{a}}_{tk} \circ \mathbf{q}_{tk} \circ \widetilde{\mathbf{a}}_{rk} \circ \mathbf{q}_{rk} \circ \widetilde{\mathbf{q}}_k + \mathcal{R}_{N_2} \end{aligned} \quad (21)$$

where

$$\widetilde{\mathbf{a}}_{tk} = \left[e^{-j\pi \frac{\widetilde{M}-1}{2} \sin(\theta_{tk})} \quad \dots \quad e^{j\pi \frac{\widetilde{M}-1}{2} \sin(\theta_{tk})} \right]^T \quad (22)$$

$$\widetilde{\mathbf{a}}_{rk} = \left[e^{-j\pi \frac{\widetilde{N}-1}{2} \sin(\theta_{rk})} \quad \dots \quad e^{j\pi \frac{\widetilde{N}-1}{2} \sin(\theta_{rk})} \right]^T \quad (23)$$

It can be found that both the transmit and the receive difference coarray can be achievable via the above-mentioned above process. Compared with (15), it is obvious that the proposed process has significantly improved the degree of freedoms.

B. Formulation of the new third tensor

It can be seen that $\widetilde{\mathbf{a}}_{tk}$ and $\widetilde{\mathbf{a}}_{rk}$ in (22) and (23) satisfy the centro-symmetric geometry, so, the DFT beamspace matrices are used to transform the complex value of $\widetilde{\mathbf{a}}_{tk}$ and $\widetilde{\mathbf{a}}_{rk}$ into the corresponding real-value ones. This operation can improve the estimation performance of the angle parameters and help to reconstruct the spatial response matrices \mathbf{Q}_t and \mathbf{Q}_r easily. Firstly, two DFT beamspace matrices are designed as

$$\mathbf{W}_t = \begin{bmatrix} \mathbf{w}_{t1}^H \\ \mathbf{w}_{t2}^H \\ \vdots \\ \mathbf{w}_{tM}^H \end{bmatrix} \quad (24)$$

Algorithm 1 pseudocode for coarray selection matrix

Input: sparse array \mathbb{S} , difference coarray \mathbb{D} , weight function \mathbb{W}

Output: coarray selection matrix \mathbf{J}

- 1: construct rectangular grid \mathbf{S}_1 and \mathbf{S}_2 via $[\mathbf{S}_1, \mathbf{S}_2] = ndgrid(\mathbb{S})$
 - 2: $\mathbf{S}_3 = \mathbf{S}_1 - \mathbf{S}_2$
 - 3: $\mathbf{S}_4 = vec(\mathbf{S}_3)$
 - 4: $\mathbf{J} = zeros(|\mathbb{D}|, |\mathbf{S}_3|)$
 - 5: **for** $i = 1 : |\mathbb{D}|$
 - 6: $[row, col] = find(\mathbf{S}_4 == \mathbb{D}(i))$
 - 7: $\mathbf{J}(i, row) = 1/\mathbb{W}(i)$
 - 8: **return** \mathbf{J}
-

$$\mathbf{W}_r = \begin{bmatrix} \mathbf{w}_{r1}^H \\ \mathbf{w}_{r2}^H \\ \vdots \\ \mathbf{w}_{r\tilde{N}}^H \end{bmatrix} \quad (25)$$

where

$$\mathbf{w}_{tm} = \left[e^{-j\frac{\pi(\tilde{M}-1)\mathbf{u}_t(m)}{\tilde{M}}} \quad \dots \quad e^{j\frac{\pi(\tilde{M}-1)\mathbf{u}_t(m)}{\tilde{M}}} \right]^T \quad (26)$$

$$m = 1, \dots, \tilde{M}$$

$$\mathbf{w}_{rn} = \left[e^{-j\frac{\pi(\tilde{N}-1)\mathbf{u}_r(n)}{\tilde{N}}} \quad \dots \quad e^{j\frac{\pi(\tilde{N}-1)\mathbf{u}_r(n)}{\tilde{N}}} \right]^T \quad (27)$$

$$n = 1, \dots, \tilde{N}$$

where $\mathbf{u}_t = [0, 1, \dots, \tilde{M}-1]$, $\mathbf{u}_r = [0, 1, \dots, \tilde{N}-1]$. Then, a 5-D tensor with real-value steering matrices can be obtained by exploiting the tensor-matrix product rules

$$\begin{aligned} \mathcal{R}_4 &= \mathcal{R}_3 \times_1 \mathbf{W}_t \times_3 \mathbf{W}_r \\ &= \sum_{k=1}^K \sigma_k^2 \hat{\mathbf{a}}_{tk} \circ \mathbf{q}_{tk} \circ \hat{\mathbf{a}}_{rk} \circ \mathbf{q}_{rk} \circ \tilde{\mathbf{q}}_k + \mathcal{R}_{N4} \end{aligned} \quad (28)$$

where $\hat{\mathbf{A}}_t = \mathbf{W}_t \tilde{\mathbf{A}}_t = [\hat{\mathbf{a}}_{t1}, \hat{\mathbf{a}}_{t2}, \dots, \hat{\mathbf{a}}_{tK}]$ and $\hat{\mathbf{A}}_r = \mathbf{W}_r \tilde{\mathbf{A}}_r = [\hat{\mathbf{a}}_{r1}, \hat{\mathbf{a}}_{r2}, \dots, \hat{\mathbf{a}}_{rK}]$ denote the real-value steering vector matrices of the transmit array and the receive array, respectively, and their detailed forms are as (29) and (30).

$$\widehat{\mathbf{A}}_t = \begin{bmatrix} \frac{\sin(\pi \frac{\widetilde{M}(\sin\theta_{t_1})}{2})}{\sin(\pi \frac{(\sin\theta_{t_1})}{2})} & \frac{\sin(\pi \frac{\widetilde{M}(\sin\theta_{t_2})}{2})}{\sin(\pi \frac{(\sin\theta_{t_2})}{2})} & \dots & \frac{\sin(\pi \frac{\widetilde{M}(\sin\theta_{t_K})}{2})}{\sin(\pi \frac{(\sin\theta_{t_K})}{2})} \\ \frac{\sin(\pi \frac{\widetilde{M}(\sin\theta_{t_1} - \frac{2\pi}{M})}{2})}{\sin(\pi \frac{(\sin\theta_{t_1} - \frac{2\pi}{M})}{2})} & \frac{\sin(\pi \frac{\widetilde{M}(\sin\theta_{t_2} - \frac{2\pi}{M})}{2})}{\sin(\pi \frac{(\sin\theta_{t_2} - \frac{2\pi}{M})}{2})} & \dots & \frac{\sin(\pi \frac{\widetilde{M}(\sin\theta_{t_K} - \frac{2\pi}{M})}{2})}{\sin(\pi \frac{(\sin\theta_{t_K} - \frac{2\pi}{M})}{2})} \\ \vdots & \vdots & \ddots & \vdots \\ \frac{\sin(\pi \frac{\widetilde{M}(\sin\theta_{t_1} - \frac{2(\widetilde{M}-1)\pi}{M})}{2})}{\sin(\pi \frac{(\sin\theta_{t_1} - \frac{2(\widetilde{M}-1)\pi}{M})}{2})} & \frac{\sin(\pi \frac{\widetilde{M}(\sin\theta_{t_2} - \frac{2(\widetilde{M}-1)\pi}{M})}{2})}{\sin(\pi \frac{(\sin\theta_{t_2} - \frac{2(\widetilde{M}-1)\pi}{M})}{2})} & \dots & \frac{\sin(\pi \frac{\widetilde{M}(\sin\theta_{t_K} - \frac{2(\widetilde{M}-1)\pi}{M})}{2})}{\sin(\pi \frac{(\sin\theta_{t_K} - \frac{2(\widetilde{M}-1)\pi}{M})}{2})} \end{bmatrix} \quad (29)$$

$$\widehat{\mathbf{A}}_r = \begin{bmatrix} \frac{\sin(\pi \frac{\widetilde{N}(\sin\theta_{r_1})}{2})}{\sin(\pi \frac{(\sin\theta_{r_1})}{2})} & \frac{\sin(\pi \frac{\widetilde{N}(\sin\theta_{r_2})}{2})}{\sin(\pi \frac{(\sin\theta_{r_2})}{2})} & \dots & \frac{\sin(\pi \frac{\widetilde{N}(\sin\theta_{r_K})}{2})}{\sin(\pi \frac{(\sin\theta_{r_K})}{2})} \\ \frac{\sin(\pi \frac{\widetilde{N}(\sin\theta_{r_1} - \frac{2\pi}{N})}{2})}{\sin(\pi \frac{(\sin\theta_{r_1} - \frac{2\pi}{N})}{2})} & \frac{\sin(\pi \frac{\widetilde{N}(\sin\theta_{r_2} - \frac{2\pi}{N})}{2})}{\sin(\pi \frac{(\sin\theta_{r_2} - \frac{2\pi}{N})}{2})} & \dots & \frac{\sin(\pi \frac{\widetilde{N}(\sin\theta_{r_K} - \frac{2\pi}{N})}{2})}{\sin(\pi \frac{(\sin\theta_{r_K} - \frac{2\pi}{N})}{2})} \\ \vdots & \vdots & \ddots & \vdots \\ \frac{\sin(\pi \frac{\widetilde{N}(\sin\theta_{r_1} - \frac{2(\widetilde{N}-1)\pi}{N})}{2})}{\sin(\pi \frac{(\sin\theta_{r_1} - \frac{2(\widetilde{N}-1)\pi}{N})}{2})} & \frac{\sin(\pi \frac{\widetilde{N}(\sin\theta_{r_2} - \frac{2(\widetilde{N}-1)\pi}{N})}{2})}{\sin(\pi \frac{(\sin\theta_{r_2} - \frac{2(\widetilde{N}-1)\pi}{N})}{2})} & \dots & \frac{\sin(\pi \frac{\widetilde{N}(\sin\theta_{r_K} - \frac{2(\widetilde{N}-1)\pi}{N})}{2})}{\sin(\pi \frac{(\sin\theta_{r_K} - \frac{2(\widetilde{N}-1)\pi}{N})}{2})} \end{bmatrix} \quad (30)$$

Afterwards, a new three way tensor \mathcal{R}_5 can be attained via combining the indices 1 and 2, 3 and 4

$$\mathcal{R}_5 = \mathcal{R}_{4[1,2][3,4][5]} = \sum_{k=1}^K \widehat{\mathbf{c}}_{tk} \circ \widehat{\mathbf{c}}_{rk} \circ \widehat{\mathbf{q}}_k + \mathcal{R}_{N5} \quad (31)$$

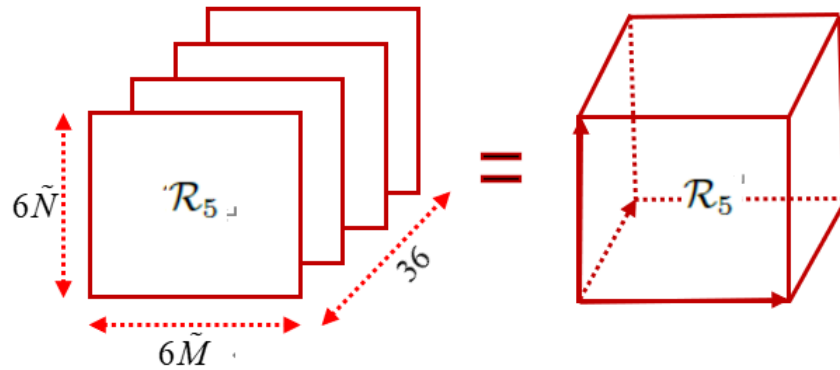


Fig. 2. The three-way tensor \mathcal{R}_5 .

As shown in Fig. 2, the dimension of the newly constructed tensor \mathcal{R}_5 is $\mathbb{C}^{6\widetilde{M} \times 6\widetilde{N} \times 36}$, whose third way is fixed at 36. On its basis, the PARAFAC algorithm can be utilized to estimate the

factor matrices $\widehat{\mathbf{C}}_t$, $\widehat{\mathbf{C}}_r$, and $\widehat{\mathbf{Q}}$, respectively. According to **Definition 6**, the different slices of the third-order tensor \mathcal{R}_5 can be further obtained as

$$\begin{aligned}\mathcal{R}_{5[i, :, :]}^T &= \widehat{\mathbf{C}}_r \mathcal{D}_i(\widehat{\mathbf{Q}}) \widehat{\mathbf{C}}_t^T, \quad i = 1, 2, \dots, 36 \\ \mathcal{R}_{5[:, j, :]}^T &= \widehat{\mathbf{Q}} \mathcal{D}_j(\widehat{\mathbf{C}}_t) \widehat{\mathbf{C}}_r^T, \quad j = 1, 2, \dots, 6\widetilde{M} \\ \mathcal{R}_{5[:, :, k]}^T &= \widehat{\mathbf{C}}_t \mathcal{D}_k(\widehat{\mathbf{C}}_r) \widehat{\mathbf{Q}}^T, \quad k = 1, 2, \dots, 6\widetilde{N}\end{aligned}\quad (32)$$

where \mathcal{D}_i , \mathcal{D}_j , \mathcal{D}_k represent the diagonal matrix operation, and the elements on the diagonal matrices are the k th-rows of the factor matrices $\widehat{\mathbf{C}}_t$, $\widehat{\mathbf{C}}_r$, and $\widehat{\mathbf{Q}}$, respectively.

In order to realize the estimation of transmit steering matrix $\widehat{\mathbf{C}}_t$, the receive steering matrix $\widehat{\mathbf{C}}_r$ and the signal matrix $\widehat{\mathbf{Q}}$, the trilinear alternating least squares algorithm is deployed as follows

$$\begin{aligned}\min_{\widehat{\mathbf{C}}_t^T} &= \|\llbracket \mathcal{R}_5^T \rrbracket_{(1)} - (\widehat{\mathbf{C}}_r \odot \widehat{\mathbf{Q}}) \widehat{\mathbf{C}}_t^T\|_F^2 \\ \min_{\widehat{\mathbf{C}}_r^T} &= \|\llbracket \mathcal{R}_5^T \rrbracket_{(2)} - (\widehat{\mathbf{Q}} \odot \widehat{\mathbf{C}}_t) \widehat{\mathbf{C}}_r^T\|_F^2 \\ \min_{\widehat{\mathbf{Q}}^T} &= \|\llbracket \mathcal{R}_5^T \rrbracket_{(3)} - (\widehat{\mathbf{C}}_t \odot \widehat{\mathbf{C}}_r) \widehat{\mathbf{Q}}^T\|_F^2\end{aligned}\quad (33)$$

Then, let $\check{\mathbf{Q}}$, $\check{\mathbf{C}}_t$ and $\check{\mathbf{C}}_r$ denote the estimated factor matrices, respectively

$$\begin{aligned}\check{\mathbf{C}}_t^T &= (\widehat{\mathbf{C}}_r \odot \widehat{\mathbf{Q}})^\dagger \llbracket \mathcal{R}_5^T \rrbracket_{(1)} \\ \check{\mathbf{C}}_r^T &= (\widehat{\mathbf{Q}} \odot \widehat{\mathbf{C}}_t)^\dagger \llbracket \mathcal{R}_5^T \rrbracket_{(2)} \\ \check{\mathbf{Q}}^T &= (\widehat{\mathbf{C}}_t \odot \widehat{\mathbf{C}}_r)^\dagger \llbracket \mathcal{R}_5^T \rrbracket_{(3)}\end{aligned}\quad (34)$$

For the factor matrices $\check{\mathbf{Q}}$, $\check{\mathbf{C}}_t$ and $\check{\mathbf{C}}_r$ obtained by multiple iterations of PARAFAC-TALS, the transmit steering matrices $\check{\mathbf{C}}_t$ and the receive steering matrices $\check{\mathbf{C}}_r$ are in one-to-one correspondence. This means that the 2D-DOD and 2D-DOA in $\check{\mathbf{C}}_t$ and $\check{\mathbf{C}}_r$ are automatically paired. Therefore, the proposed algorithm need not the construction of an additional pairing optimization function compared to the algorithms in [6]-[8].

C. Estimation of the angle and polarization parameters

For the estimated $\check{\mathbf{C}}_t$ and $\check{\mathbf{C}}_r$, the corresponding transmit elevation angle and receive elevation angle can be obtained. Firstly, structural characteristics of the steering vectors $\widehat{\mathbf{a}}_{tk}$ in $\widehat{\mathbf{A}}_t$ and $\widehat{\mathbf{a}}_{rk}$

in $\widehat{\mathbf{A}}_r$ are analyzed. The m -th and $(m+1)$ -th elements in $\widehat{\mathbf{a}}_{tk}$ and n -th and $(n+1)$ -th elements in $\widehat{\mathbf{a}}_{rk}$ can be expressed as

$$\begin{cases} [\widehat{\mathbf{a}}_{tk}]_m = \frac{\sin(\pi \frac{\widetilde{M}(\sin\theta_{tk} - \frac{2m\pi}{M})}{2})}{\sin(\pi \frac{(\sin\theta_{tk} - \frac{2m\pi}{M})}{2})} \\ [\widehat{\mathbf{a}}_{tk}]_{m+1} = \frac{\sin(\pi \frac{\widetilde{M}(\sin\theta_{tk} - \frac{2(m+1)\pi}{M})}{2})}{\sin(\pi \frac{(\sin\theta_{tk} - \frac{2(m+1)\pi}{M})}{2})} \end{cases} \quad (35)$$

$$\begin{cases} [\widehat{\mathbf{a}}_{rk}]_n = \frac{\sin(\pi \frac{\widetilde{N}(\sin\theta_{rk} - \frac{2n\pi}{N})}{2})}{\sin(\pi \frac{(\sin\theta_{rk} - \frac{2n\pi}{N})}{2})} \\ [\widehat{\mathbf{a}}_{rk}]_{n+1} = \frac{\sin(\pi \frac{\widetilde{N}(\sin\theta_{rk} - \frac{2(n+1)\pi}{N})}{2})}{\sin(\pi \frac{(\sin\theta_{rk} - \frac{2(n+1)\pi}{N})}{2})} \end{cases} \quad (36)$$

It can be seen that the adjacent elements in $\widehat{\mathbf{a}}_{tk}$ and $\widehat{\mathbf{a}}_{rk}$ satisfy the following relationships

$$\begin{aligned} \tan\left(\frac{\pi \sin(\theta_{tk})}{2}\right) \left\{ \cos\left(\frac{m\pi}{\widetilde{M}}\right) [\widehat{\mathbf{a}}_{tk}]_m + \cos\left(\frac{(m+1)\pi}{\widetilde{M}}\right) [\widehat{\mathbf{a}}_{tk}]_{m+1} \right\} \\ = \sin\left(\frac{m\pi}{\widetilde{M}}\right) [\widehat{\mathbf{a}}_{tk}]_m + \sin\left(\frac{(m+1)\pi}{\widetilde{M}}\right) [\widehat{\mathbf{a}}_{tk}]_{m+1} \end{aligned} \quad (37)$$

$$\begin{aligned} \tan\left(\frac{\pi \sin(\theta_{rk})}{2}\right) \left\{ \cos\left(\frac{n\pi}{\widetilde{N}}\right) [\widehat{\mathbf{a}}_{rk}]_n + \cos\left(\frac{(n+1)\pi}{\widetilde{N}}\right) [\widehat{\mathbf{a}}_{rk}]_{n+1} \right\} \\ = \sin\left(\frac{n\pi}{\widetilde{N}}\right) [\widehat{\mathbf{a}}_{rk}]_n + \sin\left(\frac{(n+1)\pi}{\widetilde{N}}\right) [\widehat{\mathbf{a}}_{rk}]_{n+1} \end{aligned} \quad (38)$$

On the basis of (37) and (38), the following rotation-invariant relationship for $\widehat{\mathbf{A}}_t$ and $\widehat{\mathbf{A}}_r$ can be constructed

$$\Gamma_{t1} \widehat{\mathbf{A}}_t \Phi(\theta_t) = \Gamma_{t2} \widehat{\mathbf{A}}_t \quad (39)$$

$$\Gamma_{r1} \widehat{\mathbf{A}}_r \Phi(\theta_r) = \Gamma_{r2} \widehat{\mathbf{A}}_r \quad (40)$$

where

$$\Phi(\theta_t) = \begin{bmatrix} \tan\left(\frac{\pi \sin(\theta_{t1})}{2}\right) & & & \\ & \ddots & & \\ & & \tan\left(\frac{\pi \sin(\theta_{tK})}{2}\right) & \\ & & & \end{bmatrix} \quad (41)$$

$$\Phi(\theta_r) = \begin{bmatrix} \tan\left(\frac{\pi \sin(\theta_{r1})}{2}\right) & & & \\ & \ddots & & \\ & & \tan\left(\frac{\pi \sin(\theta_{rK})}{2}\right) & \\ & & & \end{bmatrix} \quad (42)$$

The detailed forms of the selection matrices $\mathbf{\Gamma}_{t1}$, $\mathbf{\Gamma}_{t2}$, $\mathbf{\Gamma}_{r1}$, and $\mathbf{\Gamma}_{r2}$ are

$$\mathbf{\Gamma}_{t1} = \begin{bmatrix} c_{t1} & c_{t2} & 0 & \cdots & 0 \\ 0 & c_{t2} & c_{t3} & \cdots & 0 \\ 0 & 0 & c_{t3} & \cdots & 0 \\ \vdots & \vdots & \vdots & \ddots & \vdots \\ 0 & 0 & 0 & \cdots & c_{t(\widetilde{M}-1)} \end{bmatrix} \quad (43)$$

$$\mathbf{\Gamma}_{t2} = \begin{bmatrix} s_{t1} & s_{t2} & 0 & \cdots & 0 \\ 0 & s_{t2} & s_{t3} & \cdots & 0 \\ 0 & 0 & s_{t3} & \cdots & 0 \\ \vdots & \vdots & \vdots & \ddots & \vdots \\ 0 & 0 & 0 & \cdots & s_{t(\widetilde{M}-1)} \end{bmatrix} \quad (44)$$

$$\mathbf{\Gamma}_{r1} = \begin{bmatrix} c_{r1} & c_{r2} & 0 & \cdots & 0 \\ 0 & c_{r2} & c_{r3} & \cdots & 0 \\ 0 & 0 & c_{r3} & \cdots & 0 \\ \vdots & \vdots & \vdots & \ddots & \vdots \\ 0 & 0 & 0 & \cdots & c_{r(\widetilde{N}-1)} \end{bmatrix} \quad (45)$$

$$\mathbf{\Gamma}_{r2} = \begin{bmatrix} s_{r1} & s_{r2} & 0 & \cdots & 0 \\ 0 & s_{r2} & s_{r3} & \cdots & 0 \\ 0 & 0 & s_{r3} & \cdots & 0 \\ \vdots & \vdots & \vdots & \ddots & \vdots \\ 0 & 0 & 0 & \cdots & s_{r(\widetilde{N}-1)} \end{bmatrix} \quad (46)$$

where $c_{tm} = \cos(\frac{m\pi}{\widetilde{M}})$, $m = 0, 1, \dots, \widetilde{M}$, $c_{rn} = \cos(\frac{n\pi}{\widetilde{N}})$, $n = 0, 1, \dots, \widetilde{N}$, $s_{tm} = \sin(\frac{m\pi}{\widetilde{M}})$, $m = 0, 1, \dots, \widetilde{M}$, $s_{rn} = \sin(\frac{n\pi}{\widetilde{N}})$, $n = 0, 1, \dots, \widetilde{N}$. Therefore, in order to estimate the transmit elevation angle θ_{t_k} , $k = 1, 2, \dots, K$ and the receive elevation angle θ_{r_k} , $k = 1, 2, \dots, K$ in the bistatic EMVS-MIMO radar system, the following rotation-invariant relationship is further constructed

$$(\mathbf{\Gamma}_{t2} \otimes \mathbf{I}_6) \check{\mathbf{C}}_t = (\mathbf{\Gamma}_{t1} \otimes \mathbf{I}_6) \check{\mathbf{C}}_t \Phi(\theta_t) \quad (47)$$

$$(\mathbf{\Gamma}_{r2} \otimes \mathbf{I}_6) \check{\mathbf{C}}_r = (\mathbf{\Gamma}_{r1} \otimes \mathbf{I}_6) \check{\mathbf{C}}_r \Phi(\theta_r) \quad (48)$$

Then, the estimation of $\Phi(\theta_t)$ and $\Phi(\theta_r)$ can be achieved by using the least squares

$$\check{\Phi}(\theta_t) = ((\Gamma_{t1} \otimes \mathbf{I}_6) \check{\mathbf{C}}_t)^\dagger (\Gamma_{t2} \otimes \mathbf{I}_6) \check{\mathbf{C}}_t \quad (49)$$

$$\check{\Phi}(\theta_r) = ((\Gamma_{r1} \otimes \mathbf{I}_6) \check{\mathbf{C}}_r)^\dagger (\Gamma_{r2} \otimes \mathbf{I}_6) \check{\mathbf{C}}_r \quad (50)$$

Furthermore, by performing the singular value decomposition on $\check{\Phi}(\theta_t)$ and $\check{\Phi}(\theta_r)$, the corresponding eigenvalues $\lambda_{t1}, \lambda_{t2}, \dots, \lambda_{tK}$ and $\lambda_{r1}, \lambda_{r2}, \dots, \lambda_{rK}$ can be attained. Thus, the transmit elevation angle $\theta_{tk}, k = 1, 2, \dots, K$ and receive elevation angle $\theta_{rk}, k = 1, 2, \dots, K$ can be estimated as

$$\check{\theta}_{tk} = \arcsin\left(\frac{2\arctan(\lambda_{tk})}{\pi}\right), \quad k = 1, 2, \dots, K \quad (51)$$

$$\check{\theta}_{rk} = \arcsin\left(\frac{2\arctan(\lambda_{rk})}{\pi}\right), \quad k = 1, 2, \dots, K \quad (52)$$

For the estimated $\check{\theta}_{tk}, k = 1, 2, \dots, K$ and $\check{\theta}_{rk}, k = 1, 2, \dots, K$, the corresponding transmit/receive azimuth angle, transmit/receive polarization angle and transmit/receive polarization phase difference can be gained by the following process. Since the estimation process for $(\phi_{tk}, \gamma_{tk}, \eta_{tk}), k = 1, 2, \dots, K$ and $(\phi_{rk}, \gamma_{rk}, \eta_{rk}), k = 1, 2, \dots, K$ are similar, this paper only provides the comprehensive derivation process for $(\phi_{tk}, \gamma_{tk}, \eta_{tk}), k = 1, 2, \dots, K$.

By exploiting the property of Khatri-Rao product, the transmit spatial response \mathbf{Q}_t can be reconstructed as

$$\left[\mathbf{q}_{t1}, \dots, \mathbf{q}_{t1} \right] = \frac{1}{M} \sum_{m=1}^{\widetilde{M}} (\check{\mathbf{C}}_t(6m-5:6m,:)) \quad (53)$$

where $\check{\mathbf{C}}_t(6m-5:6m,:)$ denote $(6m-5)$ -th row to $6m$ -th row of $\check{\mathbf{C}}_t$. Due to the real-value transform in (28), there is no need to multiply an additional diagonal matrix when estimating the \mathbf{Q}_t , which differs from the reconstruction of \mathbf{Q}_t in [6]-[11].

For the reconstructed transmit spatial response \mathbf{Q}_t , the normalized Poynting vector corresponding to the transmit EMVS array is

$$\begin{bmatrix} \tilde{u}_{tk} \\ \tilde{v}_{tk} \\ \tilde{w}_{tk} \end{bmatrix} \triangleq \frac{\mathbf{e}_{tk}}{\|\mathbf{e}_{tk}\|} \times \frac{\mathbf{h}_{tk}^*}{\|\mathbf{h}_{tk}\|} = \begin{bmatrix} \sin(\theta_{tk}) \cos(\phi_{tk}) \\ \sin(\theta_{tk}) \sin(\phi_{tk}) \\ \cos(\theta_{tk}) \end{bmatrix} \quad (54)$$

Therefore, the estimated transmit azimuth angle $\phi_{tk}, k = 1, 2, \dots, K$ can be expressed as

$$\check{\phi}_{tk} = \arctan\left(\frac{\tilde{v}_{tk}}{\tilde{u}_{tk}}\right), \quad k = 1, 2, \dots, K \quad (55)$$

After obtaining $(\theta_{t_k}, \phi_{t_k}), k = 1, 2, \dots, K$, the corresponding transmit polarization state vector $\mathbf{g}_{t_k}(\gamma_{t_k}, \eta_{t_k})$ can be achieved

$$\mathbf{g}_{t_k}(\gamma_{t_k}, \eta_{t_k}) = \begin{bmatrix} \mathbf{g}_{1t_k} \\ \mathbf{g}_{2t_k} \end{bmatrix} = [\mathbf{F}(\check{\theta}_{t_k}, \check{\phi}_{t_k})]^\dagger \mathbf{Q}_t, \quad (56)$$

$$k = 1, 2, \dots, K$$

Consequently, the polarization parameters $(\gamma_{t_k}, \eta_{t_k}), k = 1, 2, \dots, K$ of the transmit EMVS can be obtained as

$$\check{\gamma}_{t_k} = \arctan\left[\frac{\mathbf{g}_{1t_k}}{\mathbf{g}_{2t_k}}\right], k = 1, 2, \dots, K \quad (57)$$

$$\check{\eta}_{t_k} = \angle \mathbf{g}_{1t_k}$$

Finally, the automatically paired transmit 4-D parameters $(\theta_t, \phi_t, \gamma_t, \eta_t), k = 1, 2, \dots, K$ can be gained by using the mentioned above process, and the receive 4-D parameters $(\theta_r, \phi_r, \gamma_r, \eta_r), k = 1, 2, \dots, K$ can be estimated in the same way. **Algorithm 2** offers the framework of the proposed algorithm.

D. Deterministic Cramer-Rao bound

According to [10], for a bistatic EMVS-MIMO radar with M transmit EMVS and N receive EMVS, the Cramer-Rao bound for the transmit 4-D parameters $(\boldsymbol{\theta}_t, \boldsymbol{\phi}_t, \boldsymbol{\gamma}_t, \boldsymbol{\eta}_t)$ and the receive 4-D parameters $(\boldsymbol{\theta}_r, \boldsymbol{\phi}_r, \boldsymbol{\gamma}_r, \boldsymbol{\eta}_r)$ is

$$\mathbf{CRB} = \frac{\sigma^2}{2L} [\text{real}((\mathbf{D})^H (\boldsymbol{\Pi})_{\mathbf{C}_{tr}}^\perp (\mathbf{D}) \oplus (\mathbf{R}_{ss}^T \otimes \mathbf{1}_{8 \times 8}))]^{-1} \quad (58)$$

where $\mathbf{C}_{tr} = (\mathbf{C}_t \odot \mathbf{C}_r)$ is the joint transmit-receive matrix of the bistatic EMVS-MIMO radar, $(\boldsymbol{\Pi})_{\mathbf{C}_{tr}}^\perp = \mathbf{I}_{36MN} - \mathbf{C}_{tr} \mathbf{C}_{tr}^\dagger$ denotes the projection matrix of \mathbf{C}_{tr} , \oplus denotes the Hadamard product, \mathbf{R}_{ss} represents the signal covariance matrix, $\mathbf{1}_{8 \times 8}$ is representative of the all-one matrix of dimension 8×8 , $\mathbf{D} = \left[\frac{\partial \mathbf{C}_{tr}}{\partial \boldsymbol{\theta}_t} \quad \frac{\partial \mathbf{A}}{\partial \boldsymbol{\phi}_t} \quad \frac{\partial \mathbf{C}_{tr}}{\partial \boldsymbol{\gamma}_t} \quad \frac{\partial \mathbf{C}_{tr}}{\partial \boldsymbol{\eta}_t} \quad \frac{\partial \mathbf{C}_{tr}}{\partial \boldsymbol{\theta}_r} \quad \frac{\partial \mathbf{A}}{\partial \boldsymbol{\phi}_r} \quad \frac{\partial \mathbf{C}_{tr}}{\partial \boldsymbol{\gamma}_r} \quad \frac{\partial \mathbf{C}_{tr}}{\partial \boldsymbol{\eta}_r} \right]$ is the joint derivative matrix of the \mathbf{C}_{tr} for $(\boldsymbol{\theta}_t, \boldsymbol{\phi}_t, \boldsymbol{\gamma}_t, \boldsymbol{\eta}_t)$ and $(\boldsymbol{\theta}_r, \boldsymbol{\phi}_r, \boldsymbol{\gamma}_r, \boldsymbol{\eta}_r)$.

E. Identified targets

Assume the maximum number of identified targets is K by using the proposed algorithm in this paper. The value of K is dependent on the PARAFAC algorithm, owing to the characteristic of PARAFAC decomposition, whose uniqueness, as reported in [18], can be guaranteed via the following Kruskal's theorem.

Algorithm 2 Framework of the proposed algorithm

Input: array received data matrix \mathbf{Y}

Output: the transmit 4-D parameters $(\boldsymbol{\theta}_t, \boldsymbol{\phi}_t, \boldsymbol{\gamma}_t, \boldsymbol{\eta}_t)$ and the receive 4-D parameters $(\boldsymbol{\theta}_r, \boldsymbol{\phi}_r, \boldsymbol{\gamma}_r, \boldsymbol{\eta}_r)$

- 1: construct the 5-D tensor \mathcal{Y} according to (15)
 - 2: compute the covariance tensor \mathcal{R} according to (16)
 - 3: calculate the new 5-D tensor \mathcal{R}_2 by using the tensor permutation and the generalized tensorization of the canonical polyadic decomposition according to (17) and (18)
 - 4: remove the repeated elements in the difference coarrays in \mathcal{R}_2 according to (21)
 - 5: construct the three-way tensor \mathcal{R}_5 according to (24)-(31)
 - 6: perform the PARAFAC algorithm on \mathcal{R}_5 to obtain the estimated transmit factor matrix $\widehat{\mathbf{C}}_t$ and the receive factor matrix $\widehat{\mathbf{C}}_r$ according to (32)-(34)
 - 7: construct the select matrices $\mathbf{\Gamma}_{t1}, \mathbf{\Gamma}_{t2}, \mathbf{\Gamma}_{r1}$ and $\mathbf{\Gamma}_{r2}$ to compute $\check{\check{\mathbf{\Phi}}}(\theta_t)$ and $\check{\check{\mathbf{\Phi}}}(\theta_r)$, respectively. And, by using SVD to obtain the estimated $\check{\theta}_{tk}, k = 1, 2, \dots, K$ and $\check{\theta}_{rk}, k = 1, 2, \dots, K$ according to (43)-(50)
 - 8: estimate $(\boldsymbol{\phi}_t, \boldsymbol{\gamma}_t, \boldsymbol{\eta}_t)$ by using the reconstructed matrix \mathbf{Q}_t according to (53)-(57)
 - 9: estimate the receive 3-D parameters $(\boldsymbol{\phi}_r, \boldsymbol{\gamma}_r, \boldsymbol{\eta}_r)$ by using the similar way according to step 8
 - 10: **return** $(\boldsymbol{\theta}_t, \boldsymbol{\phi}_t, \boldsymbol{\gamma}_t, \boldsymbol{\eta}_t)$ and $(\boldsymbol{\theta}_r, \boldsymbol{\phi}_r, \boldsymbol{\gamma}_r, \boldsymbol{\eta}_r)$
-

Theorem 1 (Kruskal's theorem) For a three-way tensor model $\mathcal{R}_5 \in \mathbb{C}^{6\widetilde{M} \times 6\widetilde{N} \times 36}$, the PARAFAC decomposition is unique, if

$$\kappa_{\widehat{\mathbf{C}}_t} + \kappa_{\widehat{\mathbf{C}}_r} + \kappa_{\widehat{\mathbf{Q}}} \geq 2K + 2 \quad (59)$$

where $\kappa_{\widehat{\mathbf{C}}_t}, \kappa_{\widehat{\mathbf{C}}_r}$ and $\kappa_{\widehat{\mathbf{Q}}}$ denote the κ -rank of $\widehat{\mathbf{C}}_t, \widehat{\mathbf{C}}_r$ and $\widehat{\mathbf{Q}}$, respectively. The max κ -rank of $\widehat{\mathbf{C}}_t, \widehat{\mathbf{C}}_r$ and $\widehat{\mathbf{Q}}$ are $6\widetilde{M}, 6\widetilde{N}$ and 36, respectively. Thus, the value of K can be obtained as

$$K = \frac{6\widetilde{M} + 6\widetilde{N} + 34}{2} \quad (60)$$

However, the value of K also relies on the rotation invariant relationship in (47) and (48). The maximum value of K in (47) and (48) should satisfy the following constraint

$$\begin{cases} K \leq 6(\widetilde{M} - 1) & \text{in (47)} \\ K \leq 6(\widetilde{N} - 1) & \text{in (48)} \end{cases} \quad (61)$$

According to (60) and (61), if $\widetilde{M} > \widetilde{N}$, then $K = 6(\widetilde{N} - 1)$. If $\widetilde{N} > \widetilde{M}$, then $K = 6(\widetilde{M} - 1)$. Thus, the maximum number of identified targets K is

$$K = \min[6(\widetilde{M} - 1), 6(\widetilde{N} - 1)] \quad (62)$$

Resultantly, the maximum number of identified targets is larger than the number of transmit EMVS and receive EMVS. The constructed difference coarrays in this paper are effective for the underdetermined 2D-DODs and 2D-DOAs estimation in the bistatic EMVS-MIMO radar system .

F. Computational complexity

Table I compares the main computational complexity of the proposed algorithm, the ESPRIT algorithm in [6], PM algorithm in [7], Tensor subspace-based algorithm in [8] and PARAFAC algorithm in [10]. Here, the CM, SVD and HOSVD denote the covariance matrix calculation, the singular value decomposition and the higher-order singular value decomposition, respectively. For a bistatic EMVS-MIMO radar with M transmit array and N receive array, the computational complexity of the proposed algorithm is higher than that of the PM algorithm and the PARAFAC algorithm, while lower than that of the ESPRIT algorithm and the HOSVD algorithm.

TABLE I
THE COMPUTATIONAL COMPLEXITY OF DIFFERENT ALGORITHMS.

Algorithm	the complexity of major steps				total complexity
	CM	SVD	HOSVD	multiple iterations	
ESPRIT	$(36MN)^2 L$	$(36MN)^3$	×	×	$\mathcal{O}((36MN)^2 L + (36MN)^3)$
PM	$(36MN)^2 L$	×	×	×	$\mathcal{O}((36MN)^2 L)$
Tensor	$(36MN)^2 L$	×	$4(36MN)^3$	×	$\mathcal{O}((36MN)^2 L + 4(36MN)^3)$
PARAFAC	×	×	×	$\kappa(3K^3 + 108MNKL + 3K^2(36MN + 6NL + 6ML))$	$\mathcal{O}(\kappa(3K^3 + 108MNKL + 3K^2(36MN + 6NL + 6ML)))$
Proposed	$(36MN)^2 L$	×	×	$\kappa(3K^3 + 3888\widetilde{M}\widetilde{N}K + 3K^2(36\widetilde{M}\widetilde{N} + 216\widetilde{N} + 216\widetilde{M}))$	$\mathcal{O}((36MN)^2 L + \kappa(3K^3 + 3888\widetilde{M}\widetilde{N}K + 3K^2(36\widetilde{M}\widetilde{N} + 216\widetilde{N} + 216\widetilde{M})))$

V. SIMULATION RESULTS

In order to evaluate the estimation performance of angle parameters and polarization parameters in bistatic coprime EMVS-MIMO radar, the following simulation experiments are

TABLE II
PARAMETERS OF TARGETS

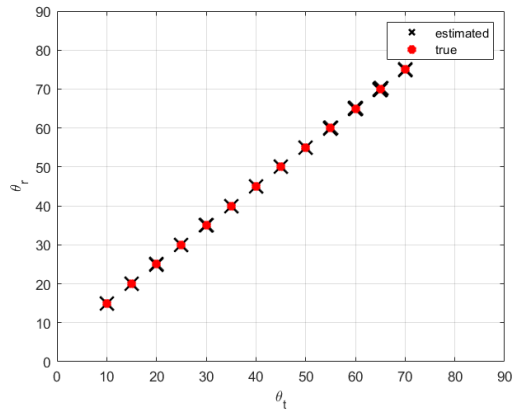
targets	θ_t/θ_r	ϕ_t/ϕ_r	γ_t/γ_r	η_t/η_r
$K = 13$	[10:5:70]	[5:5:65]	[5:3.75:50]	[3:5:63]
	[15:5:75]	[20:3.75:65]	[5:5:65]	[10:5:70]

conducted. **Firstly**, the underdetermined 2D-DODs and 2D-DOAs estimation performance is evaluated by using the proposed algorithm. Assume the number of transmit EMVS M is 9 with $(M1, M2) = (3, 4)$, the number of receive EMVS N is 10 with $(N1, N2) = (3, 5)$. The corresponding transmit 4-D parameters and receive 4-D parameters of the impinging targets are listed in Table II. Additionally, the SNR is set to 10dB, the snapshot is 200. The noise is assumed to be independent zero-mean additive Gaussian white noise, and the signal and noise are independent of each other. The scatterplot in Fig. 3 is obtained via 100 trails. Fig. 3(a) and Fig. 3(b) show that the underdetermined 2D-DODs and 2D-DOAs are accurately estimated. In the meantime, Fig. 3(c)-Fig. 3(f) demonstrate that the corresponding transmit 4-D parameters $(\theta_t, \phi_t, \gamma_t, \eta_t)$ and receive 4-D parameters $(\theta_r, \phi_r, \gamma_r, \eta_r)$ are automatically paired via the PARAFAC algorithm. Therefore, the effectiveness of proposed algorithm for the underdetermined 2D-DODs and 2D-DOAs estimation in the bistatic coprime EMVS-MIMO radar has been verified.

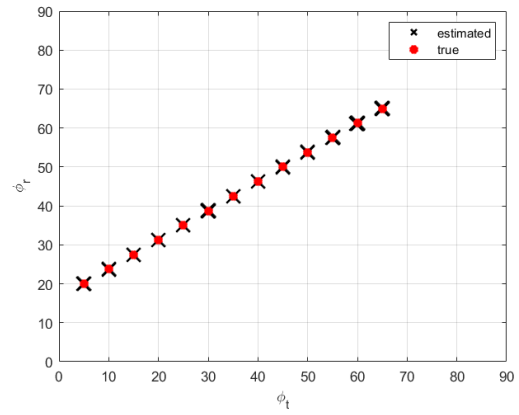
Secondly, the RMSEs performance of different algorithms versus SNR are compared. The average root mean square error (RMSE) is calculated as

$$RMSE = \sqrt{\frac{1}{KI} \sum_{i=1}^I \|\hat{\alpha} - \alpha\|^2} \quad (63)$$

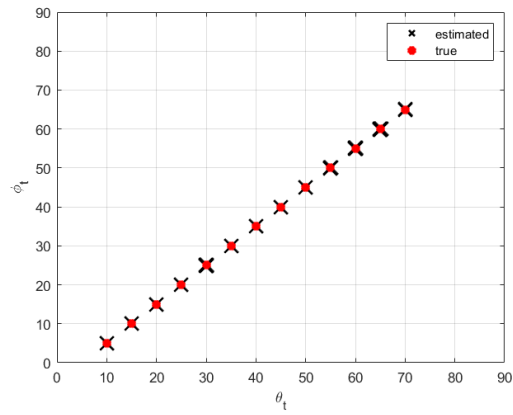
where $I = 200$ denotes the Monte Carlo trails, α and $\hat{\alpha}$ represent the true angle parameters and estimated angle parameters, respectively. Assume that there are $K = 3$ far-field targets with $\theta_t = [40^\circ, 20^\circ, 30^\circ]$, $\phi_t = [15^\circ, 25^\circ, 35^\circ]$, $\gamma_t = [10^\circ, 22^\circ, 35^\circ]$, $\eta_t = [38^\circ, 48^\circ, 56^\circ]$, $\theta_r = [24^\circ, 38^\circ, 16^\circ]$, $\phi_r = [21^\circ, 32^\circ, 55^\circ]$, $\gamma_r = [42^\circ, 33^\circ, 60^\circ]$, $\eta_r = [17^\circ, 27^\circ, 39^\circ]$, respectively. The number of SNR is increased from 0dB to 20dB and the snapshot is set to 200 for different SNRs. The suffixes 'd' and 'p' in the legend refer to angle parameter and polarization parameter, respectively. Fig. 4 shows that the proposed algorithm exhibits a better angle and polarization parameters estimation



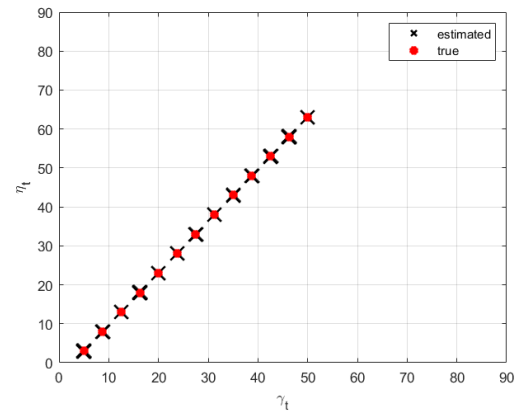
(a)



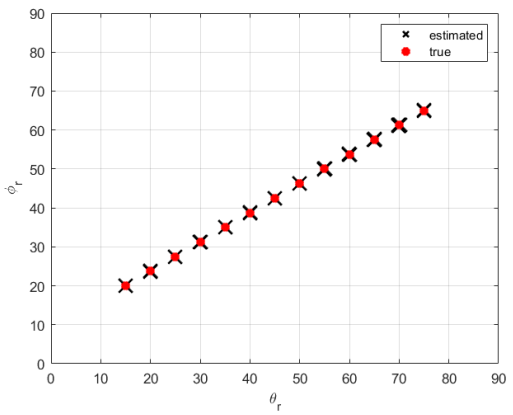
(b)



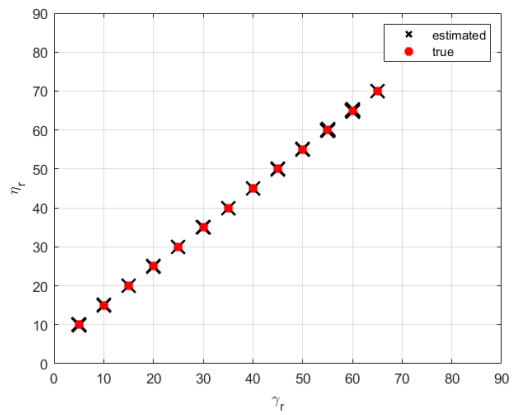
(c)



(d)



(e)



(f)

Fig. 3. Scatterplot by using the proposed method.

performance compared with the cutting-edge algorithms on the conditions of the different SNR.

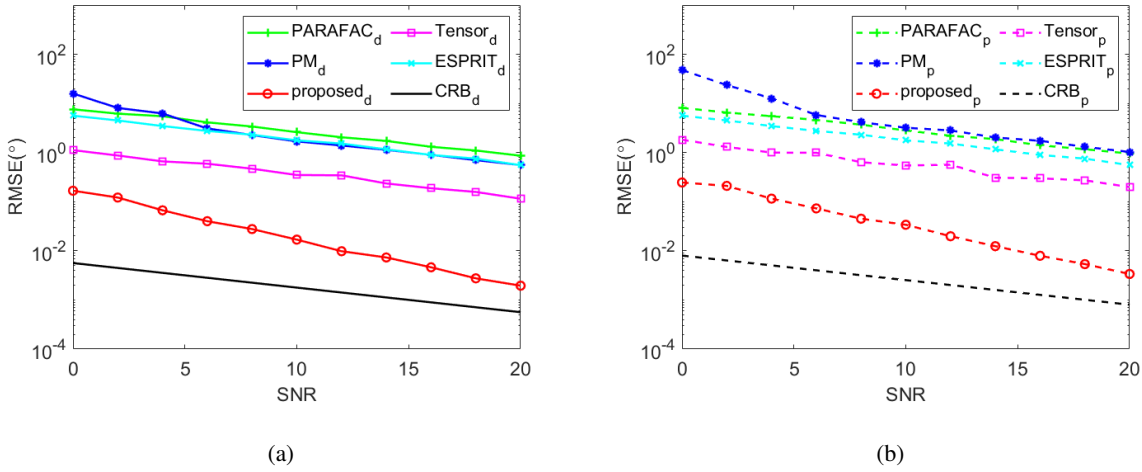


Fig. 4. RMSE versus SNR. (a) angle parameters. (b) polarization parameters.

Thirdly, the RMSEs performance of different algorithms versus the number of snapshots are assessed. The snapshots are set to vary from 100 to 1000 with a step of 100 and the SNR is fixed at $10dB$. Other simulation parameters are the same as those in the **Secondly** experiment. As evident from Fig. 5, the RMSE versus snapshots of the proposed algorithm has the smallest estimation error both for the angle parameters and polarization parameters. As a consequence, the difference coarray of the coprime EMVS used in this paper promote the angle parameters and polarization parameters estimation performance.

Fourthly, the RMSEs performance of different algorithms versus the number of impinging sources K has been compared. The number of sources vary from 2 to 8 and the corresponding transmit 4-D parameter $(\theta_t, \phi_t, \gamma_t, \eta_t)$ and receive 4-D parameters $(\theta_r, \phi_r, \gamma_r, \eta_r)$ are choosed from the Table II. The SNR and snapshots are set to $10dB$ and 200, respectively. It can be seen from Fig. 6 that the proposed method is able to maintain a reasonable estimation error for different number of sources, while the RMSEs for the other three algorithms become large with the increase of K . This phenomenon indicates that the proposed algorithm is robust to the different number of sources.

Finally, the estimation performance of the two closely-located targets has been evaluated by using the proposed method. Here, the biases between the true angle/polarization parameters and the mean of estimated angle/polarization parameters versus SNR and snapshots are examined.

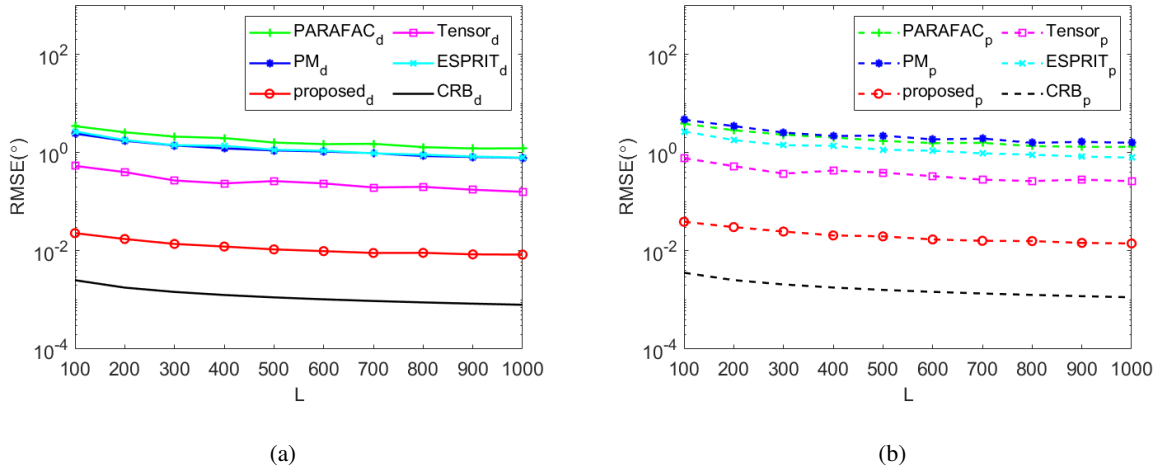


Fig. 5. RMSE versus snapshot. (a) angle parameters. (b) polarization parameters.

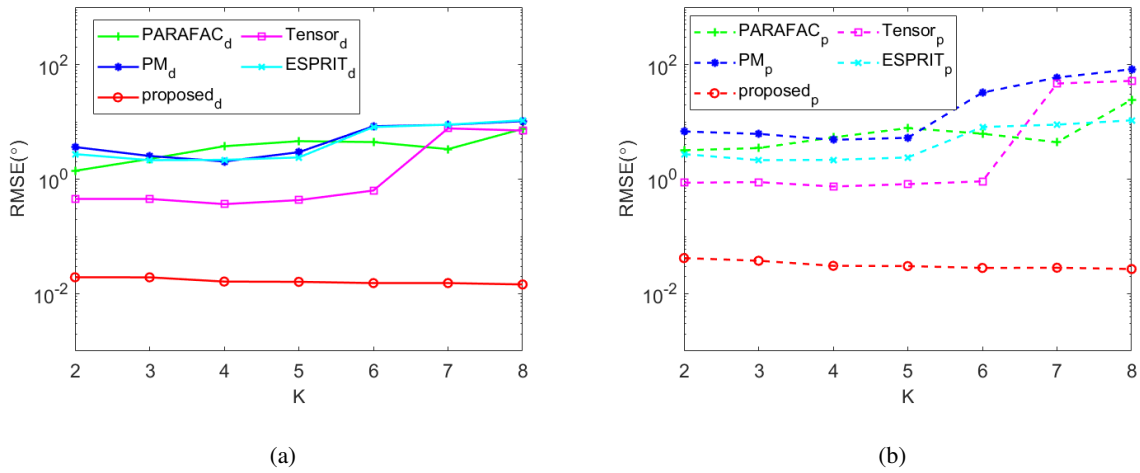


Fig. 6. RMSE versus K . (a) angle parameters. (b) polarization parameters.

The transmit 4-D parameters and receive 4-D parameters of the two closely located targets are set to $\boldsymbol{\theta}_t = [22^\circ, 23^\circ]$, $\boldsymbol{\phi}_t = [26^\circ, 28^\circ]$, $\boldsymbol{\gamma}_t = [45^\circ, 55^\circ]$, $\boldsymbol{\eta}_t = [53^\circ, 63^\circ]$, $\boldsymbol{\theta}_r = [33^\circ, 35^\circ]$, $\boldsymbol{\phi}_r = [34^\circ, 36^\circ]$, $\boldsymbol{\gamma}_r = [20^\circ, 65^\circ]$, $\boldsymbol{\eta}_r = [28^\circ, 47^\circ]$, respectively. As illustrated in Fig. 7, the estimated bias by the proposed method is very small with the increase of SNR/snapshots.

VI. CONCLUSION

A tensor-based algorithm has been investigated to deal with the underdetermined 2D-DOD and 2D-DOA estimation in the bistatic EMVS-MIMO radar system, and its effectiveness has been well verified via simulations. This algorithm is advantageous to the realization of de-coupling

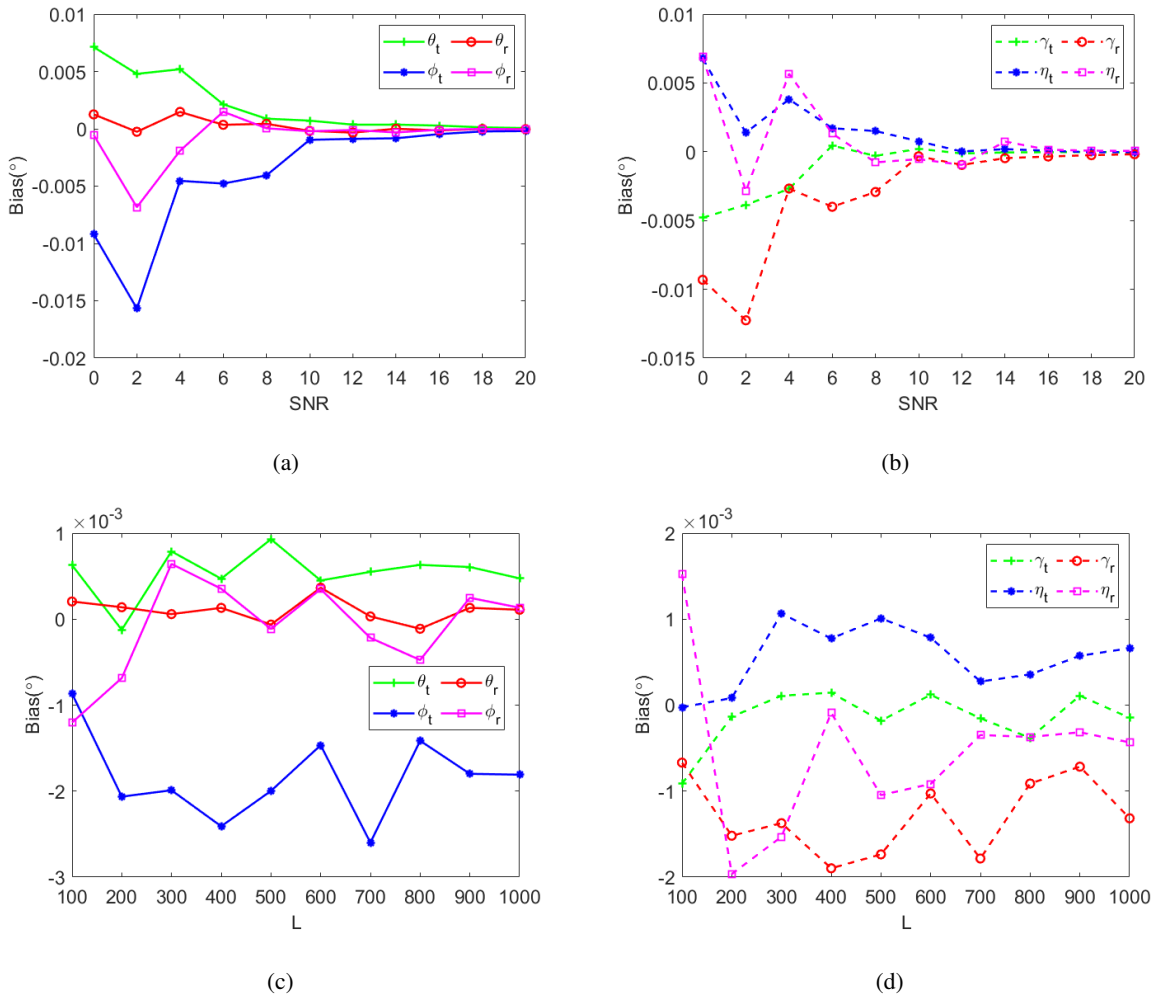


Fig. 7. Bias performance of the proposed method for the two closely-located targets. (a) angle bias versus SNR . (b) polarization bias versus SNR. (c) angle bias versus snapshot . (d) polarization bias versus snapshot.

between the spatial response and steering matrix, and it also contributes to the difference coarrays construction of transmit and receive EMVS, which plays an important role to estimate more targets than elements. More meaningfully, a variety of newly-designed sparse arrays in recent research can also be used as the transmit/receive EMVS in the bistatic MIMO radar system and this method can pave a path to obtain the corresponding difference coarrays to enhance the estimation performance.

REFERENCES

[1] Wong K.T, Song Y, Fulton C. J, et al, "Electrically "Long" Dipoles in a Collocated/Orthogonal Trial-for Direction Finding and Polarization Estimation," *IEEE Transactions on Antennas and Propagation*, vol. 65,no. 11 pp. 6057-6067, 2017.

- [2] Khan S, Wong K.T, “Electrically Long Dipoles in a Crossed Pair for Closed-Form Estimation of an Incident Source’s Polarization,” *IEEE Transactions on Antennas and Propagation*, vol. 67, no. 8, pp. 5569-5581, 2019.
- [3] Khan S, Wong K.T, Song Y, Tam W.Y, “Electrically Large Circular Loops in the Estimation of an Incident Emitter’s Direction-of-Arrival or Polarization,” *IEEE Transactions on Antennas and Propagation*, vol. 66, no. 6, pp. 3046-3055, 2019.
- [4] Khan S, Wong K.T, “A Six-Component Vector Sensor Comparising Electrically Long Dipoles and Large Loops-to Simultaneously Estimate Incident Sources’ Direction-of-Arrival and Polarizations,” *IEEE Transactions on Signal Processing*, vol. 68, no.8, pp.6355-6363, 2020.
- [5] Lan X, Liu W, Ngan H, “Joint DOA and Polarisation Estimation with Crossed-dipole and Tripole Sensor Arrays,” *IEEE Transactions on Aerospace and Electronic Systems*, vol. 56, no. 6, pp. 4965-4973, 2020.
- [6] Chintagunta S, Ponnusamy P. “2D-DOD and 2D-DOA estimation using the electromagnetic vector sensors,” *Signal Processing*, vol. 147, pp. 163-172, 2018.
- [7] Liu T, Wen F, Shi J, et al, “A Computationally Economic Location Algorithm for Bistatic EMVS-MIMO radar,” *IEEE ACCESS*, vol. 7, pp.120533-120540, 2019.
- [8] Mao C, Shi J, Wen F, “Target Localization in Bistatic EMVS-MIMO radar using Tensor Subspace Method,” *IEEE ACCESS*, vol. 7, pp. 163119-1632127, 2019.
- [9] Wen F, Shi J, “Fast direction finding for bistatic EMVS-MIMO radar without pairing,” *Signal Processing*, vol. 173, pp.10512, 2020.
- [10] Wen F, Shi J, Zhang Z, “Joint 2D-DOD, 2D-DOA, and Polarization Angles Estimation for Bistatic EMVS-MIMO Radar via PARAFAC Analysis,” *IEEE Transactions on Vehicular Technology*, vol. 69, no. 2, pp. 1626-1638, 2020.
- [11] Xianpeng Wang, Mengxing Huang, Liangtian Wan, “Joint 2D-DOD and 2D-DOA estimation for Coprime EMVS-MIMO radar,” *Circuits, Systems, and Signal Processing*, vol. 40, pp. 2950-2966, 2021.
- [12] Vaidyanathan P.P, Pal P, “Sparse sensing with co-prime samplers and arrays,” *IEEE Transactions on Signal Processing*, vol. 59,no.2, pp. 573-586, 2011.
- [13] Liu C, Vaidyanathan P P, Pal P, “Coprime coarray interpolation for DOA estimation via nuclear norm minimization,” *IEEE International Symposium on Circuits and Systems, Montreal,*, Canada, pp. 2639-2642, 2016.
- [14] Zhou C, Gu Y, Fan X, et al, “Direction of arrival estimation for coprime array via virtual array interpolation,” *IEEE Transactions on Signal Processing*, vol. 66, no.22, pp.5956-5971, 2018.
- [15] Shi J, Hu G, Zhang X, et al , “Sparsity-based 2D DOA estimation for coprime array: From sun-difference coarray viewpoint,” *IEEE Transactions on Signal Processing*, vol. 65, no. 21, pp.5591-5604, 2017.
- [16] Hang Zheng, Zhiguo Shi, Chengwei Zhou, Martin Haardt, Jian Chen, “Coupled Coarray Tensor CPD for DOA Estimation With Coprime L-Shaped Array,” *IEEE Signal Processing Letters* , vol. 28, pp.1545-1549, 2021.
- [17] Hang Zheng, Chengwei Zhou, Yong Wang, Jinfang Zhou, Zhiguo Shi, “Sample Fourth-order Cumulant Tensor Denoising for DOA Estimation with Coprime L-shaped Array,” *2021 55th Asilomar Conference on Signals, Systems, and Computers*, Pacific Grove, CA, 2021.
- [18] T. G. Kolda and B. W. Bader, “Tensor decompositions and applications ,” *SIAM Rev*, vol. 51, no. 3, pp. 455–500, 2009.
- [19] Cichocki, Danilo Mandic, Lieven De Lathauwer, et al, “Tensor Decompositions for Signal Processing Applications: From two-way to multiway component analysis,” *IEEE Signal Processing Magazine* , vol. 32, no. 2, pp. 145-163, 2015.
- [20] Nicholas D. Sidiropoulos, Lieven De Lathauwer, et al, “Tensor Decomposition for Signal Processing and Machine Learning,” *IEEE Transactions on Signal Processing*, vol. 65, no. 13, pp.3551-3582, 2017.
- [21] W. Rao, D. Li, and J. Zhang, “A tensor-based approach to L-shaped arrays processing with enhanced degrees of freedom,” *IEEE Signal Process. Lett.*, vol. 25, no. 2, pp. 1-5, 2018.

- [22] Donghe Liu, Yongbo Zhao, Chenghu Cao, Xiaojiao Pang, "A novel reduced-dimensional beamspace unitary ESPRIT algorithm for monostatic MIMO radar," *Digital Signal Processing* , vol. 40, pp. 2950-2966, 2021.
- [23] Jianshu Zhang, Damir Rakhimov, Martin Haardt, "Gridless Channel estimation for hybrid mmWave MIMO systems via Tensor-ESPRIT algorithms in DFT Beamspace," *IEEE Journal of Selected Topics in Signal Processing*, vol. 15, no. 3, pp. 816-831, 2021.
- [24] Feng Xu, Sergiy A. Vorobyov, Fawei Yang, "Transmit Beamspace DDMA Based Automotive MIMO Radar," *IEEE Transactions on Vehicular Technology* , vol. 71, no. 2, pp. 1669-1684, 2022.
- [25] Sheng Chen, Yongbo Zhao, Yili Hu, Xiaojiao Pang, "A beamspace maximum likelihood algorithm for target height estimation for a bistatic MIMO radar," *Digital Signal Processing* , vol. 122, pp. 103330, 2022.
- [26] Sheng Chen, Yongbo Zhao, Yili Hu, "Beamspace Phase Solving Algorithm for Elevation Angle Estimation," *IEEE Signal Processing Letters* , vol. 29, pp. 742-746, 2022.